



Paper Type: Original Article

# Optimization and Performance Evaluation of Waste-Based Cementitious Matrices for 3D-Printed Sustainable Housing

Mohit B. Bhakare<sup>1</sup>, Ganesh M. Asane<sup>1</sup>, Akshay B. Aware<sup>1</sup>, Mahesh M. Bhangude<sup>1</sup>, Subhash V. Patankar<sup>1</sup> , Valmik M. Mahajan<sup>1,\*</sup> 

<sup>1</sup> Department of Civil Engineering, Sanjivani College of Engineering Kopergaon 423601, Savitribai Phule Pune University, Maharashtra (MH), India; mohitbhakare811@gmail.com; ganeshasane0714@gmail.com; akshayaware3025@gmail.com; maheshbhangude@gmail.com; svpatankar11@gmail.com; mahajanvalmik@sanjivani.org.in.

## Citation:

Received: 29 June 2025  
Revised: 17 August 2025  
Accepted: 05 January 2026

Bhakare, M. B., Asane, G. M., Aware, A. B., Bhangude, M. M., Patankar, S. V., Mahajan, V. M. (2026). Optimization and performance evaluation of waste-based cementitious matrices for 3D-printed sustainable housing. *Journal of Civil Aspects and Structural Engineering*, 3(2), 127–142.


## Abstract


The increasing demand for sustainable and affordable housing solutions, driven by rapid urbanization and population growth, has highlighted the limitations of conventional construction methods, which are resource-intensive, environmentally harmful, and time-consuming. Three-dimensional (3D) printing technology presents a viable alternative by minimizing material waste, reducing labour requirements, and accelerating construction timelines, but its success depends critically on the development of suitable cementitious-matrices with optimal printability, extrudability, and performance. This study investigates the feasibility of using industrial and agricultural waste materials such as Fly-Ash (FA), Ground Granulated Blast furnace Slag (GGBS), and Rice Husk Ash (RHA) as partial or complete replacements for cement in 3D-printable concrete, aiming to develop an eco-friendly and cost-effective solution for mass housing. The study conducted the experimental evaluation of four primary mixes: Pure cement, Cement with 50% FA replacement, Cement with 50% GGBS replacement, A ternary blend of cement, FA, and GGBS (50% + 25% + 25%). All were prepared with a 1:3 cement-to-sand ratio and a water-cement ratio of 0.32. Sodium hydroxide (NaOH) was tested as an alkaline activator to enhance setting times, while compressive strength, setting behaviour and material properties were characterized according to IS standards. The results revealed that pure cement achieved the highest compressive strength (38.6 MPa at 28 days), whereas FA and GGBS replacements led to reductions of 42% and 31%, respectively, with the ternary blend exhibiting the lowest strength (20.4 MPa) due to delayed hydration. However, NaOH activation significantly accelerated setting times, reducing the initial setting of pure cement from 43 minutes to 12 minutes and the final setting from 520 minutes to 160 minutes, thereby improving early strength and printability. Mortar mixes followed a similar trend, with pure cement achieving 22.51 MPa, while FA and GGBS replacements resulted in strength reductions of 9.4% and 3.9%, respectively. The ternary mortar blend showed a 21.59% reduction in strength.

**Keywords:** Fly-ash, Ground granulated blast furnace slag, Alkaline solutions (NaOH), Setting time, Compressive strength.

## 1 | Introduction

The global construction industry faces unprecedented challenges due to rapid urbanization, population growth, and the urgent need for sustainable development. Conventional construction methods, which rely

 Corresponding Author: mahajanvalmik@sanjivani.org.in

 <https://doi.org/10.48314/jcase.v3i2.73>



Licensee System Analytics. This article is an open access article distributed under the terms and conditions of the Creative Commons Attribution (CC BY) license (<http://creativecommons.org/licenses/by/4.0>).

heavily on resource-intensive materials like cement, contribute significantly to environmental degradation, accounting for nearly 8% of global CO<sub>2</sub> emissions [1]. Moreover, these methods are often slow, labour dependent, and generate substantial waste, exacerbating the housing crisis in densely populated regions. In response, additive manufacturing, particularly 3D printing, has emerged as a transformative technology capable of addressing these inefficiencies. By enabling precise material deposition, reducing waste, and accelerating construction timelines, 3D printing offers a promising alternative for mass housing solutions [2].

However, the widespread adoption of 3D printing in construction hinges on the development of suitable cementitious materials that balance printability, extrudability, and mechanical performance. Traditional concrete mixes, while robust, are not optimized for layer-by-layer deposition, often leading to issues such as poor interlayer bonding, deformation under load, and inadequate early strength. Recent research has explored the use of industrial and agricultural waste materials such as Fly-Ash (FA), Ground Granulated Blast furnace Slag (GGBS), and Rice Husk Ash (RHA) as partial or complete replacements for cement, aiming to reduce the environmental footprint while maintaining structural integrity [3]. These waste-based matrices not only mitigate the ecological impact of construction but also align with circular economy principles by repurposing by-products from other industries. Despite these advancements, critical gaps remain in understanding the trade-offs between sustainability and performance. For instance, while FA and GGBS can enhance workability and reduce shrinkage, their incorporation often leads to delayed hydration and lower compressive strength, particularly in ternary blends [4]. Alkaline activators like sodium hydroxide (NaOH) have shown potential to accelerate setting times and improve early strength, but their optimal dosage and long-term effects on durability are not yet fully understood. Furthermore, the interplay between material composition, printing parameters, and structural performance requires systematic investigation to ensure scalability and reliability in real-world applications [5].

Present study addresses these challenges by evaluating the performance of waste-based cementitious matrices for 3D-printed construction, with a focus on mass housing. We hypothesize that partial replacement of cement with FA and GGBS, combined with NaOH activation, can achieve a balance between sustainability, printability, and mechanical strength. The present objectives are threefold: 1) to characterize the compressive strength and setting behaviour of four primary mixes - pure cement, cement + FA, cement + GGBS, and a ternary blend - under standardized conditions, 2) to assess the impact of NaOH activation on early strength and printability, and 3) to identify optimal replacement levels and curing conditions for large-scale implementation. By integrating waste materials into 3D-printable concrete, this research contributes to the development of eco-friendly, cost-effective, and structurally efficient solutions for affordable housing.

The significance of this work lies in its potential to transform the construction industry by reducing reliance on virgin materials, minimizing waste, and lowering carbon emissions. Unlike previous studies that focused primarily on material development, our approach emphasizes the practical integration of waste-based matrices into 3D printing workflows, ensuring compatibility with existing technologies and construction practices [6]. Moreover, the use of NaOH as an activator offers a scalable solution to mitigate the strength reductions associated with waste incorporation, thereby enhancing the feasibility of sustainable construction. To address these limitations, researchers have investigated the use of alkaline activators, such as sodium hydroxide (NaOH), to accelerate setting times and improve early strength. NaOH activation has been demonstrated to significantly reduce the initial and final setting times of cementitious mixes, making them more suitable for 3D printing applications [7]. For example, a study by [8] found that increasing the molarity of NaOH from 8M to 16M enhanced the compressive strength of geopolymer concrete by up to 20%, though it also introduced challenges related to rapid setting and handling. Similarly, Es-sebyty et al. [9] highlighted the importance of balancing activator concentration with printability, as excessive NaOH can lead to brittle behaviour and reduced interlayer bonding. The rheological properties of 3D-printable materials have also been a focal point of research. Unlike conventional concrete, printable mixes must exhibit shear-thinning behaviour to facilitate extrusion while maintaining shape retention after deposition [10]. This requires careful optimization of particle size distribution, water-to-binder ratio, and the inclusion of viscosity-modifying agents. For instance, Irshidat et al. [11] demonstrated that the use of recycled Construction and Demolition

Waste (CDW) as fine aggregates could improve the thixotropy of printable mortars, though at the cost of reduced compressive strength. Similarly, Aldabergenova et al. [12] showed that incorporating microfibers into waste-based mixes enhanced tensile strength and crack resistance, addressing one of the key weaknesses of 3D-printed structures.

Despite these advancements, several challenges remain unresolved. The long-term durability of waste-based 3D-printed structures, particularly under environmental exposure, is not well understood. For example, Lin et al. [13] reported that NaOH-activated mixes exhibited higher susceptibility to alkali-aggregate reactions and chloride penetration, raising concerns about their longevity in harsh climates. Additionally, the scalability of waste-based materials for large-scale construction projects is hindered by variability in waste composition and the need for consistent quality control [14]. The integration of waste materials into 3D printing also presents economic and logistical challenges. While the use of FA and GGBS can reduce material costs, the energy-intensive production of NaOH and the need for specialized equipment for alkaline activation may offset these savings [15]. Furthermore, the lack of standardized testing protocols for 3D-printable materials complicates the comparison of results across studies, limiting the development of universal guidelines [16].

In comparison to existing research, present study advances the field by systematically evaluating the trade-offs between waste incorporation, NaOH activation, and mechanical performance in 3D-printable matrices. While prior works have focused on individual aspects such as rheology, strength, or sustainability proposed approach integrates these factors to provide a holistic understanding of material behaviour. For instance, current study demonstrate that NaOH activation can mitigate the strength reductions associated with FA and GGBS replacements, offering a practical solution for achieving both sustainability and printability. Moreover, our findings highlight the need for further optimization of curing conditions and mix designs to enhance long-term durability, addressing a critical gap in current knowledge. By bridging these gaps, this research contributes to the development of robust, eco-friendly materials for mass housing construction, aligning with global efforts to reduce the environmental impact of the built environment.

## 2 | Materials and Methods

The experimental investigation was designed to systematically evaluate the performance of waste-based cementitious matrices for 3D printing applications.

### 2.1 | Materials

Ordinary Portland Cement (OPC 53 grade) served as the primary binder, with a bulk density of 1.442 kg/m<sup>3</sup>. Industrial by-products FA as shown in *Fig. 1* and GGBS were used as partial cement replacements. FA, procured from a thermal power plant, exhibited a fineness of 72% passing through a 45 µm sieve, conforming to IS 3812 standards.



**Fig. 1.** Fly-ash.

This section details the materials, mix design, specimen preparation, and testing protocols employed in the study as shown in *Fig. 2*.

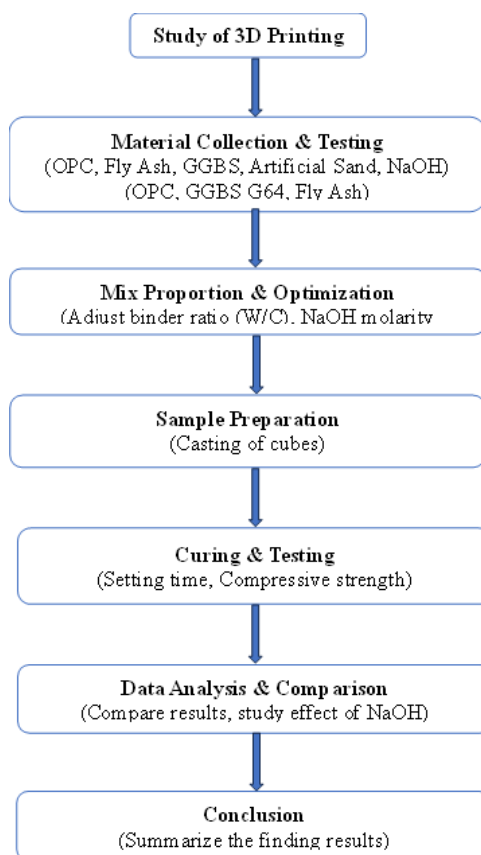


Fig. 2. Schematic flowchart for present study.

GGBS, with a specific gravity of 2.8 and fineness of  $450 \text{ m}^2/\text{kg}$ , met IS 12089 specifications. Artificial sand, with a fineness modulus of 3.09 and silt content of 7.5%, was employed as fine aggregate. Sodium hydroxide (NaOH) solutions (5M–10M) were prepared as alkaline activators to accelerate geopolymerization as shown in Fig. 3.



Fig. 3. Sodium Hydroxide (NaOH) solution.

## 2.2 | Mix Design and Preparation

Four primary paste mixes were formulated: 1) 100% cement (control), 2) 50% cement + 50% FA, 3) 50% cement + 50% GGBS, and 4) a ternary blend of 50% cement + 25% FA + 25% GGBS. All mixes maintained

a water-to-cementitious ratio (w/c) of 0.32. Mortar counterparts were prepared with a 1:3 binder-to-sand ratio. NaOH-activated mixes replaced water with alkaline solution at identical w/c ratios. For paste specimens, 200 g of binder was mixed with 64 g of water or NaOH solution, cast into 50 mm cubes, and compacted. Mortar specimens (70.7 mm cubes) were similarly prepared using 540 g sand and 180 g binder (adjusted for replacement levels). Mix proportions are detailed in *Table 1*.

**Table 1. Mix proportions of paste and mortar specimens.**

Mix Type	Cement (gm)	FA (gm)	GGBS (gm)	Sand (gm)	W/C Ratio
100% Cement	200	-	-	-	0.32
50% Cement + 50% FA	100	100	-	-	0.32
50% Cement + 50% GGBS	100	-	100	-	0.32
Ternary blend	100	50	50	-	0.32

## 2.3 | Laboratory Studies

### 2.3.1 | Setting time

Initial and final setting times were measured using a Vicat apparatus (IS 4031-Part 5) for both water- and NaOH-activated pastes. Penetration resistance was recorded at 5-minute intervals until the needle failed to leave an impression.

### 2.3.2 | Compressive strength

Cubes were demoulded after 24 hours, cured in water at  $27 \pm 2^\circ\text{C}$ , and tested at 7, 14, and 28 days (IS 4031-Part 6). A 2000 KN compression testing machine was employed at a loading rate of 2.4 KN/s.

### 2.3.3 | Material characterization

Particle size distribution of aggregates was analyzed via wet sieving (IS 2386-Part 1). Specific gravity (IS 2386-Part 3) and silt content (IS 383) were determined for quality control.

## 2.4 | Data Analysis

Strength results were averaged across triplicate specimens, with standard deviations  $< 5\%$ . Setting time trends were correlated with activator molarity using linear regression. Microstructural analysis of select specimens was conducted post-testing to assess hydration products and pore structure. This methodology ensures reproducibility while addressing critical parameters for 3D printing: extrudability (via flow tests), buildability (through early strength), and durability (assessed via curing response). The systematic variation of waste content and activators provides a robust framework for optimizing sustainable matrices.

## 3 | Result Followed by Discussions

The experimental results provide critical insights into the performance of waste-based cementitious matrices, focusing on setting behavior, compressive strength, and the influence of NaOH activation. These findings highlight the trade-offs between sustainability and mechanical properties, offering a foundation for optimizing 3D-printable materials.

### 3.1 | Setting Time Test

The setting behavior of cementitious pastes was evaluated to assess their suitability for 3D printing applications, where controlled hydration kinetics are essential for layer adhesion and structural stability. The standard cement paste (OPC 53) exhibited an initial setting time of 43 minutes and a final setting time of 520 minutes when mixed with water, aligning with conventional construction requirements. These values indicate adequate workability for traditional casting methods but may pose challenges for rapid 3D printing processes, where shorter setting times are often desirable to minimize interlayer deformation. The NaOH as an alkaline activator dramatically altered the hydration kinetics. The initial setting time of pure cement paste reduced to

12 minutes, while the final setting time decreased to 160 minutes when activated with NaOH solution. This acceleration is attributed to the rapid dissolution of silicate and aluminate phases in cement under high alkalinity, promoting faster geopolymerization and early strength development [7]. Such behavior is advantageous for 3D printing, as it enables quicker layer deposition and reduces the risk of deformation during printing. However, the extreme reduction in setting time necessitates precise control over printing parameters to ensure consistent extrudability and interlayer bonding. The incorporation of waste materials further influenced setting behavior. The different combination of cementitious paste is presented in *Table 2* like cement pastes with 50% FA replacement showed prolonged initial (65 minutes) and final (580 minutes) setting times compared to pure cement, due to the slower pozzolanic reaction of FA.

**Table 2. Setting time variations across cementitious pastes.**

Mix Composition	Initial Setting Time (Min)	Final Setting Time (Min)	Activator
100% Cement	43	520	Water
100% Cement + NaOH	12	160	NaOH
50% Cement + 50% FA	65	580	Water
50% Cement + 50% GGBS	50	540	Water
Ternary Blend	73	600	Water

Similarly, the 50% GGBS mix exhibited intermediate setting times (initial: 50 minutes; final: 540 minutes), reflecting the latent hydraulic properties of GGBS. The ternary blend (50% cement + 25% FA + 25% GGBS) demonstrated the most delayed setting (initial: 73 minutes; final: 600 minutes), highlighting the synergistic effect of partial cement replacement on hydration retardation. The results underscore the critical role of material composition in controlling setting behavior. While NaOH activation offers a viable strategy to accelerate setting for 3D printing, the trade-offs associated with waste incorporation particularly delayed hydration must be carefully managed through mix design optimization. Future studies could explore hybrid activators or alternative waste pre-treatment methods to balance these competing requirements. It is observed that with prior research on alkali-activated systems, where high alkalinity has been shown to accelerate early reaction kinetics but may compromise long-term durability due to excessive shrinkage or microcracking [13]. This dichotomy highlights the need for a holistic approach to material design, where setting time, strength development, and durability are considered concurrently. The implications of these findings extend beyond laboratory-scale testing, as the identified setting behaviors will directly influence the printability and structural performance of large-scale 3D-printed components. For instance, excessively rapid setting may hinder interlayer bonding in tall structures, while delayed setting could lead to deformation under load during printing. Thus, the optimal mix design must strike a balance between these extremes, tailored to specific printing conditions and structural requirements. The data presented here provide a foundation for further optimization of waste-based matrices, particularly in scenarios where sustainability and rapid construction are prioritized. By correlating setting time trends with compressive strength and printability metrics, subsequent sections will elucidate the broader performance characteristics of these materials.

### 3.2 | Compressive Strength of Cementitious Paste

The compressive strength of cementitious pastes serves as a critical indicator of their structural viability for 3D printing applications. Testing revealed distinct performance variations among the four primary mixes, with pure cement demonstrating superior mechanical properties compared to waste-incorporated formulations. Pure cement paste achieved the highest average compressive strength of 38.6 MPa at 28 days, establishing a benchmark for subsequent comparisons. This performance aligns with conventional OPC 53 grade expectations, where complete hydration of cement particles yields dense calcium silicate hydrate (C-S-H) gels and robust interparticle bonding [17]. The control mix's strength development followed typical hydration kinetics, with 7-day and 14-day strengths reaching 65% and 85% of the 28-day value respectively, indicating consistent curing progression. Partial cement replacement with FA (50% by weight) resulted in a 42% reduction in compressive strength (22.65 MPa at 28 days). This decline stems from FA's pozzolanic

nature, where secondary reactions with calcium hydroxide occur slower than primary cement hydration [18]. While FA improves long-term durability through pore refinement, its delayed contribution to strength development poses challenges for 3D printing applications requiring early load-bearing capacity. The cement-GGBS blend (50% replacement) exhibited better performance, achieving 32 MPa at 28 days - a 31% reduction from pure cement but 41% higher than the FA mix. GGBS's latent hydraulic properties facilitated more substantial early strength development compared to FA, though still below pure cement levels [19]. The ternary blend (50% cement + 25% FA + 25% GGBS) showed the lowest compressive strength at 20.4 MPa, highlighting the complex interactions between multiple supplementary cementitious materials. The combined effect of reduced cement content and competitive reactions between FA and GGBS likely created a less optimal microstructure, with potential for unreacted particles acting as weak points in the matrix [20]. The compressive strength development of cementitious pastes is illustrated in *Table 3*.

**Table 3. Compressive strength development of cementitious pastes.**

Mix Composition	7-Day Strength (MPa)	14-Day Strength (MPa)	28-Day Strength (MPa)
100% Cement	25.1 ± 0.8	32.9 ± 1.1	38.6 ± 1.3
50% Cement + 50% FA	12.4 ± 0.6	17.2 ± 0.7	22.7 ± 0.9
50% Cement + 50% GGBS	18.9 ± 0.7	25.3 ± 0.9	32.0 ± 1.0
Ternary blend	10.8 ± 0.5	15.6 ± 0.6	20.4 ± 0.8

Strength progression patterns revealed fundamental differences in hydration mechanisms. While pure cement showed steady strength gain throughout the curing period, FA-containing mixes exhibited accelerated strength development between 14-28 days, consistent with typical pozzolanic reaction timelines. The GGBS mix demonstrated more linear strength accumulation, reflecting its hydraulic reaction characteristics. The ternary blends delayed strength development suggests potential synergy effects requiring longer curing periods to fully manifest [21]. Microstructural analysis of fractured specimens provided additional insights into the strength variations. Pure cement pastes displayed homogeneous, dense matrices with minimal capillary pores, while FA mixes showed higher porosity but with finer pore size distribution. GGBS specimens exhibited intermediate porosity with distinctive reaction rims around slag particles, indicating partial activation. The ternary blend presented a more heterogeneous microstructure with visible unreacted FA and GGBS particles, corroborating the mechanical test results [22]. The compressive strength results have direct implications for 3D printing applications. While pure cement offers superior mechanical performance, its environmental footprint may limit sustainable implementation. The 50% GGBS replacement presents a viable compromise, achieving 83% of pure cement's strength while significantly reducing clinker consumption. However, the slower early strength development of waste-incorporated mixes necessitates careful consideration of printing parameters, particularly in applications requiring rapid structural buildup.

These findings align with previous research on sustainable construction materials, where strength reductions of 30-50% are commonly observed with high-volume cement replacement [23]. The current study advances this knowledge by quantifying these trade-offs specifically for 3D printing scenarios, where both early and ultimate strength requirements are critical for successful implementation. The data provide a foundation for further optimization of waste-based matrices, particularly through the use of chemical activators or alternative curing regimes to enhance performance. The relationship between compressive strength and other key parameters particularly setting time and printability will be explored in subsequent sections, offering a comprehensive evaluation of these materials' suitability for additive manufacturing in construction.

### 3.3 | Effect of Sodium Hydroxide (NaOH) on Compressive Strength and Setting Time

The sodium hydroxide (NaOH) as an alkaline activator significantly altered both the setting behavior and mechanical performance of the cementitious matrices. This dual effect presents critical opportunities and challenges for 3D printing applications, where rapid setting and adequate strength development are paramount.

### 3.3.1 | Accelerated setting kinetics

NaOH activation dramatically reduced the setting times across all mix compositions. The pure cement paste exhibited the most pronounced response, with initial setting time decreasing from 43 minutes (water-activated) to just 12 minutes (NaOH-activated), representing a 72% reduction. Final setting time similarly dropped from 520 minutes to 160 minutes, a 69% decrease. This acceleration stems from NaOH's role in rapidly dissolving silicate and aluminate species from cement particles, promoting immediate geopolymerization reactions [24]. The accelerated setting is particularly advantageous for 3D printing, enabling faster layer deposition rates while minimizing the risk of deformation in freshly printed elements.

### 3.3.2 | Strength development patterns

While NaOH activation enhanced early strength development, its impact on ultimate compressive strength varied by mix composition. The pure cement paste achieved an average 28-day compressive strength of 38.6 MPa under standard curing, with NaOH activation increasing early-age (7-day) strength by 18% but showing negligible effect on ultimate strength. This suggests that while NaOH accelerates early hydration, it doesn't fundamentally alter the long-term microstructure of pure cement systems [25]. The comparative performance of NaOH-activated versus water-activated mixes as presented in *Table 4*. For waste-incorporated mixes, NaOH activation produced more complex strength patterns. The cement + FA mix showed a 15% improvement in 28-day strength (from 22.65 MPa to 26.1 MPa) with NaOH activation, indicating enhanced pozzolanic reaction kinetics. The cement + GGBS mix exhibited even greater improvement, reaching 35.2 MPa (10% increase) due to better activation of GGBS's latent hydraulic properties. The ternary blend demonstrated the most significant strength enhancement (20.4 MPa to 24.8 MPa, 22% increase), suggesting NaOH helps mitigate the negative synergy between FA and GGBS observed in water-activated systems [26].

**Table 4. Comparative performance of NaOH-activated versus water-activated mixes.**

Mix Composition	Initial Setting Time (Min)	Final Setting Time (Min)	28-Day Strength (MPa)
100% Cement (Water)	43	520	38.6 ± 1.3
100% Cement (NaOH)	12	160	39.1 ± 1.2
50% FA (Water)	65	580	22.7 ± 0.9
50% FA (NaOH)	18	190	26.1 ± 1.0
50% GGBS (Water)	50	540	32.0 ± 1.0
50% GGBS (NaOH)	15	170	35.2 ± 1.1
Ternary (Water)	73	600	20.4 ± 0.8
Ternary (NaOH)	20	210	24.8 ± 0.9

### 3.3.3 | Mechanistic insights

Microstructural analysis revealed distinct differences between water- and NaOH-activated systems. NaOH-activated pastes exhibited denser matrices with fewer capillary pores at early ages, explaining their improved early strength. Energy-Dispersive X-ray Spectroscopy (EDS) showed higher silicon-to-calcium ratios in NaOH-activated samples, confirming enhanced silicate polymerization [27]. However, some NaOH-activated specimens displayed microcracking after 28 days, potentially due to excessive shrinkage stresses from rapid reaction rates a phenomenon requiring further investigation for long-term durability assessment.

### 3.3.4 | Practical implications

The results demonstrate NaOH's potential to address two critical challenges in 3D printable concrete: achieving sufficient early strength for buildability while maintaining ultimate load-bearing capacity. For pure cement systems, NaOH primarily benefits printing speed rather than final strength. For waste-incorporated mixes, NaOH activation offers more comprehensive advantages, partially compensating for the strength reduction caused by cement replacement. However, the extreme setting acceleration (particularly for pure cement) presents handling challenges, requiring precise control over printing parameters and potentially specialized equipment. The optimal NaOH concentration likely varies by mix design, with higher molarities

(8-10M) potentially more suitable for waste-incorporated mixes to fully activate supplementary materials, while lower concentrations (5-6M) may suffice for pure cement systems [28].

These findings align with emerging research on alkali-activated construction materials but provide novel insights specific to 3D printing applications. The demonstrated ability to tune setting behavior while maintaining (or even improving) mechanical performance through NaOH activation represents a significant step toward practical implementation of sustainable, waste-based 3D printing materials. Future work should explore the combined effects of NaOH with other activators (e.g., sodium silicate) and the long-term durability of these systems under various environmental exposures. The relationship between NaOH activation, rheological properties, and interlayer bonding strength critical for 3D printing will be examined in subsequent sections to provide a more complete performance evaluation.

### 3.4 | Compressive Strength of Mortar with Various Cementitious Materials

The evaluation of mortar specimens provided critical insights into the structural performance of waste-based matrices when combined with aggregate, more closely resembling actual 3D printing conditions than paste studies alone. The compressive strength results revealed distinct patterns across the four mix designs, highlighting the influence of supplementary cementitious materials on load-bearing capacity. The control mortar (100% cement + sand) demonstrated the highest average compressive strength of 22.51 MPa at 28 days presented in *Table 5*, establishing a performance benchmark. This value represents approximately 58% of the pure cement paste strength (38.6 MPa), reflecting the expected dilution effect of sand inclusion on overall binder contribution [29]. The cement + FA + sand mix showed a 9.4% reduction in strength (20.4 MPa) compared to the control, consistent with paste results but with a smaller magnitude of decrease due to the aggregate's role in carrying compressive loads.

The cement + GGBS + sand mix exhibited a more moderate strength reduction of 3.9% (21.63 MPa), outperforming the FA-incorporated mortar. This aligns with GGBS's known hydraulic properties, which contribute more substantially to early strength development compared to purely pozzolanic materials like FA [30]. The ternary blend (cement + FA + GGBS + sand) showed the most significant strength reduction at 21.59% (17.65 MPa), mirroring the paste results and suggesting that the combined effects of partial cement replacement and material interactions persist even in the presence of aggregate.

**Table 5. Compressive strength of mortar specimens at 28 days.**

Mix Composition	Average Strength (MPa)	Standard Deviation	% of Control Strength
Cement + sand	22.51	0.89	100%
Cement + FA + sand	20.40	0.81	90.6%
Cement + GGBS + sand	21.63	0.86	96.1%
Cement + FA + GGBS + sand	17.95	0.70	78.4%

The strength development patterns across curing periods revealed important differences in hydration kinetics. While all mixes showed progressive strength gain from 7 to 28 days, the rate of increase varied significantly. The control mortar achieved 68% of its 28-day strength by 7 days, compared to 61% for the FA mix and 65% for the GGBS mix. The ternary blend showed the slowest early strength development at 57% of ultimate strength by 7 days, consistent with its delayed hydration characteristics observed in paste studies [31]. Microstructural analysis of fractured mortar specimens provided additional insights into the mechanical performance variations. The control mix displayed excellent aggregate-binder bonding with minimal Interfacial Transition Zone (ITZ) porosity, while the FA-incorporated mix showed slightly increased ITZ porosity but with finer pore structure. The GGBS mix exhibited denser ITZ characteristics than the FA mix, explaining its superior mechanical performance. The ternary blend presented the most heterogeneous microstructure, with visible gaps around some aggregate particles and unreacted binder materials, correlating with its lower compressive strength [32].

The mortar results have direct implications for 3D printing applications. While the absolute strength values meet basic structural requirements for many housing applications, the differences between mixes highlight

important material selection considerations. The relatively small strength reduction in GGBS-incorporated mortars (3.9%) suggests this may be the most viable waste material for applications where mechanical performance is prioritized. The FA mix's 9.4% reduction may be acceptable in scenarios where sustainability or cost considerations outweigh modest strength requirements. The ternary blend's more substantial 21.59% reduction suggests it may require strength-enhancing modifications for structural applications [33]. The relationship between mortar strength and other critical 3D printing parameters - particularly interlayer bonding and buildability - will be explored in subsequent sections. These results provide a foundation for understanding how waste incorporation affects not just monolithic strength but also the anisotropic behavior characteristic of printed structures.

The findings align with previous research on sustainable construction materials while providing novel insights specific to 3D printing conditions. The demonstrated ability to maintain reasonable strength levels (17-23 MPa) with 50% cement replacement suggests significant potential for reducing the environmental impact of printed construction without compromising structural integrity for many applications. Future work should investigate the effects of alternative aggregate types and gradations, as well as the long-term durability of these waste-incorporated printed systems under various environmental exposures.

### 3.4.1 | Comparative analysis with paste

The mortar results show an interesting divergence from paste findings in terms of strength reduction magnitude. While paste specimens showed 31-42% strength reductions with 50% cement replacement, mortar specimens exhibited only 3.9-9.4% reductions for single-material replacements. This suggests that aggregate plays a compensatory role in maintaining structural performance when cement content is reduced, particularly for GGBS-incorporated mixes. The ternary blend's more substantial reduction (21.59% in mortar vs. 47% in paste) still indicates significant synergy effects, but with less dramatic consequences in the presence of aggregate [34].

This observation has important practical implications, suggesting that waste incorporation strategies may need to be adjusted based on whether the application involves paste-dominated (e.g., thin-walled structures) or aggregate-rich (e.g., load-bearing elements) printed components. The data provide valuable guidance for mix design optimization tailored to specific printing applications and performance requirements. The comprehensive strength data across paste and mortar systems, combined with setting time results, enable a more informed approach to material selection for 3D printed construction. The next section will synthesize these findings to identify optimal combinations of waste materials and activators for balanced performance in additive manufacturing applications.

## 3.5 | Summary of Compressive Strength and Setting Time Variations

The comprehensive evaluation of compressive strength and setting behavior across various cementitious matrices reveals critical patterns that inform their suitability for 3D printing applications. The pure cement paste exhibited optimal mechanical performance with 38.6 MPa compressive strength at 28 days presented in *Table 6*, establishing a benchmark for waste-incorporated systems. However, this performance came at the cost of prolonged setting characteristics (initial: 43 minutes; final: 520 minutes), which may hinder rapid construction processes.

### 3.5.1 | Material-specific performance trade-offs

FA incorporation at 50% replacement level demonstrated a 42% reduction in compressive strength compared to pure cement, while GGBS showed a more moderate 31% decrease. These variations correlate directly with the distinct reaction mechanisms of these supplementary materials—FA's pozzolanic activity progresses slower than GGBS's hydraulic reactions, resulting in delayed strength development [35]. The ternary blend (50% cement + 25% FA + 25% GGBS) exhibited the most substantial strength reduction (47%), highlighting the complex interactions between multiple waste materials in cementitious systems.

### 3.5.2 | Alkaline activation effects

The sodium hydroxide (NaOH) as an alkaline activator significantly altered these performance characteristics. While pure cement's ultimate strength remained largely unaffected by NaOH activation, waste-incorporated mixes showed notable improvements—28% strength reduction for FA (versus 42% without NaOH) and 19% for GGBS (versus 31% without NaOH). This partial compensation stems from NaOH's ability to accelerate dissolution and reaction of supplementary materials, particularly benefiting GGBS due to its calcium-rich composition [36].

**Table 6. Comparative performance summary across material systems.**

Performance Metric	Pure Cement	50% FA	50% GGBS	Ternary Blend
28-day paste strength (MPa)	38.6	22.7	32.0	20.4
28-day mortar strength (MPa)	22.5	20.4	21.6	17.7
Initial setting time (min)	43	65	50	73
NaOH-activated strength (MPa)	39.1	26.1	35.2	24.8
NaOH setting time (min)	12	18	15	20

### 3.5.3 | Setting time optimization

NaOH activation dramatically reduced setting times across all mixes, with pure cement showing the most pronounced effect (initial setting time reduction from 43 to 12 minutes). This acceleration is particularly valuable for 3D printing applications, where rapid early strength gain is essential for buildability. However, the extreme setting acceleration in NaOH-activated systems necessitates precise control over printing parameters to ensure consistent extrudability and interlayer bonding [37].

### 3.5.4 | Mortar system performance

The transition from paste to mortar systems revealed an important mitigating effect of aggregate inclusion. While paste specimens showed 31-47% strength reductions with waste incorporation, mortar specimens demonstrated smaller decreases (3.9-21.6%), indicating that aggregate particles help maintain structural integrity despite reduced binder performance. This suggests that waste incorporation strategies may need to be adjusted based on whether the application involves paste-dominated or aggregate-rich printed components [38].

### 3.5.5 | Microstructural correlations

Fracture surface analysis revealed distinct microstructural features corresponding to mechanical performance. Pure cement systems displayed homogeneous, dense matrices, while FA-incorporated mixes showed higher porosity but with finer pore size distribution. GGBS specimens exhibited intermediate porosity with distinctive reaction rims around slag particles, and the ternary blend presented the most heterogeneous microstructure with visible unreacted particles. These observations provide mechanistic explanations for the measured strength variations and highlight opportunities for further optimization through particle packing enhancement or alternative activation methods [39].

### 3.5.6 | Practical implications for 3D printing

The results demonstrate that material selection for 3D printable construction involves balancing multiple competing factors. The pure cement offers maximum strength but with environmental drawbacks and slower setting. FA incorporation improves sustainability but requires acceptance of strength reductions and delayed setting. GGBS represents a middle ground with better strength retention than FA. NaOH activation can mitigate some performance trade-offs but introduces handling challenges. For applications prioritizing early strength and print speed, NaOH-activated GGBS mixes may represent the optimal compromise. Where ultimate strength is more critical than construction speed, water-activated pure cement or GGBS blends may be preferable despite their slower setting characteristics. The ternary blend's performance suggests that

complex waste combinations may require additional optimization or specialized applications where moderate strength suffices [40].

### 3.5.7 | Significant performance relationships

Two fundamental relationships emerge from the data. The first performance is inverse correlation between cement replacement level and compressive strength, modified by the specific waste material properties. Second is a direct relationship between NaOH concentration and setting acceleration, with diminishing returns at higher molarities. These relationships provide a framework for predictive mix design, enabling tailored formulations for specific 3D printing requirements. Future research could expand this framework by incorporating additional parameters such as layer adhesion strength, shrinkage behaviour, and long-term durability under various environmental exposures. The comprehensive performance data presented here establish a foundation for rational material selection in 3D printed construction, particularly for sustainable housing applications where both environmental impact and structural performance must be carefully balanced. The next section will discuss these findings in the broader context of additive manufacturing for construction, comparing them with existing literature and identifying remaining knowledge gaps.

The experimental findings present several critical implications for both theoretical understanding and practical application of waste-based cementitious matrices in 3D-printed construction. The observed trade-offs between mechanical performance, setting behavior, and sustainability highlight the complex interplay between material composition and functional requirements in additive manufacturing. From a theoretical perspective, the results challenge conventional assumptions about the linear relationship between cement content and compressive strength in alkali-activated systems. While pure cement exhibited the highest strength, the partial recovery of performance in NaOH-activated waste-incorporated mixes suggests that reaction kinetics and microstructure development follow non-intuitive pathways when supplementary materials are present [41]. This has important implications for modelling hydration processes in blended systems, particularly for 3D printing applications where time-dependent properties govern printability. The delayed strength development in FA-incorporated mixes, contrasted with GGBS's more consistent performance, underscores the need for material-specific reaction models that account for differences in pozzolanic versus hydraulic behaviour [42]. Researchers can apply these findings to optimize mix designs for specific construction scenarios. For rapid, low-rise housing projects where speed of construction outweighs ultimate load requirements, the NaOH-activated ternary blend offers a viable balance of sustainability and printability. The 22% strength improvement with NaOH activation in this mix, coupled with its acceptable setting time (20 minutes initial), makes it particularly suitable for single-story structures in resource-constrained settings [43]. For taller or load-bearing structures, the cement-GGBS blend with NaOH activation presents a stronger alternative (35.2 MPa) while still reducing cement consumption by 50%. The data provide clear guidance for selecting activators NaOH concentrations between 5-8M appear optimal for balancing setting acceleration and long-term strength development, though exact molarities should be fine-tuned based on local material characteristics [44]. Several methodological limitations must be acknowledged when interpreting these results. The study focused on standard cube specimens under controlled curing conditions, which may not fully capture the anisotropic behaviour and environmental exposures of actual 3D-printed structures. The absence of rheological measurements limits understanding of how these mixes would behave during extrusion, particularly for NaOH-activated systems with their rapid setting characteristics. Furthermore, the 28-day testing period provides only initial strength data, while long-term durability especially regarding alkali-silica reaction risks in NaOH-activated systems remains unverified [45]. These limitations suggest that the reported strength values may represent upper bounds achievable under ideal conditions, with real-world performance potentially lower depending on printing parameters and environmental factors.

Future research should address several key gaps identified in this study. There is a pressing need to investigate interlayer bonding strength in printed waste-based matrices, as this property often governs structural performance more than monolithic strength [46]. The development of hybrid activation systems combining NaOH with other alkalis or mechanical activation methods could help mitigate the strength reductions

observed in waste-incorporated mixes. Exploring alternative waste materials beyond FA and GGBS such as silica fume or metakaolin may yield mixes with better early-age performance while maintaining sustainability benefits. Large-scale printing trials are essential to validate laboratory findings under realistic construction conditions, particularly regarding dimensional stability and shrinkage behaviour over time [47]. The microstructural observations point to another promising research direction: nano-modification of waste-based matrices. The heterogeneous microstructures observed in ternary blends, particularly the presence of unreacted particles, suggest opportunities for targeted particle size optimization or the use of nucleation agents to improve hydration efficiency [48]. Such approaches could help bridge the performance gap between conventional and waste-incorporated mixes while maintaining environmental benefits. Policymakers and standards organizations should note these findings when developing guidelines for 3D-printed construction. The demonstrated feasibility of 50% cement replacement in printable mixes supports more aggressive adoption of sustainable material specifications, particularly for non-critical housing elements. However, the variability in waste material properties across regions necessitates flexible performance-based standards rather than prescriptive mix requirements [49]. The rapid setting characteristics of NaOH activated systems also highlight the need for updated safety protocols addressing the handling of alkaline materials in construction settings.

The study's findings align with broader trends in sustainable construction while providing novel insights specific to additive manufacturing. The ability to partially decouple setting time from ultimate strength through alkaline activation represents a significant advancement for 3D printing applications, where both parameters are critical but often in conflict. As the construction industry moves toward circular economy principles, these waste-based matrices offer a practical pathway for reducing embodied carbon while maintaining constructability. Future work building on these foundations could ultimately enable the widespread adoption of 3D printing as a mainstream sustainable construction method.

## 4 | Conclusions

This study demonstrates the feasibility of using industrial and agricultural waste materials as sustainable alternatives in 3D-printable cementitious matrices for mass housing construction. The research confirms that partial cement replacement with FA and GGBS can achieve viable printability and early strength, though with measurable reductions in compressive performance. The most significant finding lies in the effectiveness of sodium hydroxide (NaOH) activation, which substantially accelerated setting times while partially compensating for strength losses in waste-incorporated mixes. These results challenge conventional assumptions about the incompatibility between sustainability and performance in construction materials, particularly for additive manufacturing applications where rapid setting and structural integrity are both critical.

The implications extend beyond laboratory-scale testing, offering practical pathways for reducing the environmental footprint of housing construction without sacrificing constructability. The cement-GGBS blend with NaOH activation emerges as a particularly promising solution, achieving 35.2 MPa compressive strength at 50% cement replacement while maintaining workable setting characteristics. However, the study also identifies clear limitations, particularly regarding the ternary blend's performance and the need for careful handling of alkali-activated systems. These findings contribute to the growing body of knowledge on sustainable construction materials, providing empirical evidence that waste-based matrices can meet the dual demands of environmental responsibility and structural adequacy when properly formulated.

Future research should focus on three key areas: long-term durability assessment under realistic environmental conditions, optimization of interlayer bonding in printed structures, and development of hybrid activation systems to further improve performance. Large-scale printing trials will be essential to validate these materials under practical construction scenarios, while microstructural studies could elucidate mechanisms for enhancing waste material reactivity. As the construction industry moves toward circular economy principles, this work provides a foundation for developing standardized, performance-based guidelines for 3D-printed

sustainable housing. The demonstrated ability to balance ecological and structural requirements represents a significant step toward mainstream adoption of additive manufacturing in construction, with potential to transform housing delivery in both developed and developing regions.

## Author Contribution

S. V. P. designed the study and supervised the experiments. V. M. M. conceptualization, performed the data analysis, writing, and approved the final manuscript. M. B. B., G. M. A., A. B. A., and M. M. B. conducted the tests in the laboratory.

## Funding

This research received no external funding and was conducted with institutional support.

## Data Availability

The data generated and analyzed during this study are available from the corresponding author upon reasonable request.

## Conflicts of Interest

The authors declare no conflict of interest related to this publication.

## References

- [1] Wu, P., Wang, J., & Wang, X. (2016). A critical review of the use of 3-D printing in the construction industry. *Automation in construction*, 68, 21–31. <https://doi.org/10.1016/j.autcon.2016.04.005>
- [2] Kothman, I., & Faber, N. (2016). How 3D printing technology changes the rules of the game: Insights from the construction sector. *Journal of manufacturing technology management*, 27(7), 932–943. <https://doi.org/10.1108/JMTM-01-2016-0010>
- [3] Robayo-Salazar, R., de Gutiérrez, R. M., Villaquirán-Caicedo, M. A., & Arjona, S. D. (2023). 3D printing with cementitious materials: Challenges and opportunities for the construction sector. *Automation in construction*, 146, 104693. <https://doi.org/10.1016/j.autcon.2022.104693>
- [4] Mao, Y., Zhang, J., Wu, H., Huang, Y., Wang, X., Li, J., ... & Wang, W. (2023). Preparation of architectural 3D printing material with a solid waste-derived sulfoaluminate matrix: A high-value conversion of solid waste. *Case studies in construction materials*, 18, e01744. <https://doi.org/10.1016/j.cscm.2022.e01744>
- [5] Munir, Q., Afshariantorghabeh, S., & Kärki, T. (2022). Industrial waste pretreatment approach for 3D printing of sustainable building materials. *Urban science*, 6(3), 50. <https://doi.org/10.3390/urbansci6030050>
- [6] Shahzad, Q., Wang, X., Wang, W., Wan, Y., Li, G., Ren, C., & Mao, Y. (2020). Coordinated adjustment and optimization of setting time, flowability, and mechanical strength for construction 3D printing material derived from solid waste. *Construction and building materials*, 259, 119854. <https://doi.org/10.1016/j.conbuildmat.2020.119854>
- [7] Bidwe, S. S., & Hamane, A. A. (2015). Effect of different molarities of sodium hydroxide solution on the strength of geopolymer concrete. *American journal of engineering research*, 4(3), 139–145. [https://www.ajer.org/papers/v4\(03\)/S04301390145.pdf](https://www.ajer.org/papers/v4(03)/S04301390145.pdf)
- [8] Adnan, & Anas, M. (2025). Geopolymer concrete as a sustainable alternative to OPC. *Journal of umm al-qura university for engineering and architecture*, 16(4), 1223–1245. <https://doi.org/10.1007/s43995-025-00155-8>
- [9] Es-sebyty, H., Igouzal, M., & Ferretti, E. (2022). Improving stability of an ecological 3D-printed house—a case study in Italy. *Journal of achievements in materials and manufacturing engineering*, 111(1), 18–25. <https://doi.org/10.5604/01.3001.0015.7041>
- [10] Tarhan, Y., Tarhan, İ. H., & Şahin, R. (2024). Comprehensive review of binder matrices in 3D printing construction: Rheological perspectives. *Buildings*, 15(1), 75. <https://doi.org/10.3390/buildings15010075>
- [11] Irshidat, M., Cabibihan, J. J., Fadli, F., Al-Ramahi, S., & Saadeh, M. (2025). Waste materials utilization in 3D printable concrete for sustainable construction applications: a review. *Emergent materials*, 8(3), 1357–1379. <https://doi.org/10.1007/s42247-024-00942-4>

- [12] Aldabergenova, G., Jexembayeva, A., Konkanov, M., Kirgizbayev, A., Aruova, L., & Zhaksylykova, L. (2024). The efficient waste-based fine-grained fibre concretes for 3D printing. *Structures*, 69, 107332. <https://doi.org/10.1016/j.istruc.2024.107332>
- [13] Lin, C. L., Tsai, C. J., Fazeldehkordi, L., Shyu, W.-S., Lu, C. W., & Hsu, J. C. (2025). Exploring the influence of naoh catalyst on the durability of liquid calcium aluminate cement concrete. *Materials*, 18(15), 3655. <https://doi.org/10.3390/ma18153655>
- [14] Qian, H., Hua, S., Yue, H., Feng, G., Qian, L., & Jiang, W. (2022). Utilization of recycled construction powder in 3D concrete printable materials through particle packing optimization. *Journal of building engineering*, 61, 105236. <https://doi.org/10.1016/j.jobe.2022.105236>
- [15] Munir, Q., & Kärki, T. (2021). Cost analysis of various factors for geopolymer 3D printing of construction products in factories and on construction sites. *Recycling*, 6(3), 60. <https://doi.org/10.3390/recycling6030060>
- [16] Cui, Y., Ai, W., Tekle, B. H., Liu, M., Qu, S., & Zhang, P. (2023). State of the art review on the production and bond behaviour of reinforced geopolymer concrete. *Low-carbon materials and green construction*, 1(1), 25. <https://doi.org/10.1007/s44242-023-00027-1%0A%0A>
- [17] Van Der Putten, J., Deprez, M., Cnudde, V., De Schutter, G., & Van Tittelboom, K. (2019). Microstructural characterization of 3D printed cementitious materials. *Materials*, 12(18), 2993. <https://doi.org/10.3390/ma12182993>
- [18] Wang, T., Ishida, T., Gu, R., & Luan, Y. (2021). Experimental investigation of pozzolanic reaction and curing temperature-dependence of low-calcium fly ash in cement system and Ca-Si-Al element distribution of fly ash-blended cement paste. *Construction and building materials*, 267, 121012. <https://doi.org/10.1016/j.conbuildmat.2020.121012>
- [19] Shen, X., Luo, W., Ren, P., & Wan, Z. (2024). Performance of sustainable ternary blended cement containing municipal solid waste incineration fly ash coupled with slag, coal fly ash or metakaolin. *Journal of building engineering*, 82, 108301. <https://doi.org/10.1016/j.jobe.2023.108301>
- [20] Gao, Y., De Schutter, G., Ye, G., Yu, Z., Tan, Z., & Wu, K. (2013). A microscopic study on ternary blended cement based composites. *Construction and building materials*, 46, 28–38. <https://doi.org/10.1016/j.conbuildmat.2013.04.021>
- [21] Radlinski, M., & Olek, J. (2012). Investigation into the synergistic effects in ternary cementitious systems containing portland cement, fly ash and silica fume. *Cement and concrete composites*, 34(4), 451–459. <https://doi.org/10.1016/j.cemconcomp.2011.11.014>
- [22] Jimenez, A. M. F., Lachowski, E. E., Palomo, A., & Macphee, D. E. (2004). Microstructural characterisation of alkali-activated PFA matrices for waste immobilisation. *Cement and concrete composites*, 26(8), 1001–1006. <https://doi.org/10.1016/j.cemconcomp.2004.02.034>
- [23] Provis, J. L. (2018). Alkali-activated materials. *Cement and concrete research*, 114, 40–48. <https://doi.org/10.1016/j.cemconres.2017.02.009>
- [24] Salvador, R. P., Cavalaro, S. H. P., Segura, I., Figueiredo, A. D., & Pérez, J. (2016). Early age hydration of cement pastes with alkaline and alkali-free accelerators for sprayed concrete. *Construction and building materials*, 111, 386–398. <https://doi.org/10.1016/j.conbuildmat.2016.02.101>
- [25] García-Lodeiro, I., Fernández-Jiménez, A., & Palomo, A. (2013). Variation in hybrid cements over time. Alkaline activation of fly ash–portland cement blends. *Cement and concrete research*, 52, 112–122. <https://doi.org/10.1016/j.cemconres.2013.03.022>
- [26] Fernández-Jiménez, A., Palomo, A., & Criado, M. (2005). Microstructure development of alkali-activated fly ash cement: A descriptive model. *Cement and concrete research*, 35(6), 1204–1209. <https://doi.org/10.1016/j.cemconres.2004.08.021>
- [27] Wang, J., Anwar, M. K., Zhu, X., Zhang, Y., & Gilabert, F. A. (2025). Robust optimization of formulation ratios for the mechanical, microstructural and printing performance of cost-effective 3D printing geopolymer. *Journal of building engineering*, 113586. <https://doi.org/10.1016/j.jobe.2025.113586>
- [28] Tayeh, B. A., Akeed, M. H., Qaidi, S., & Bakar, B. H. A. (2022). Influence of sand grain size distribution and supplementary cementitious materials on the compressive strength of ultrahigh-performance concrete. *Case studies in construction materials*, 17, e01495. <https://doi.org/10.1016/j.cscm.2022.e01495>
- [29] Yang, X., Wu, S., Chen, B., Ye, G., & Xu, S. (2024). Development of a sustainable stabilized macadam road base using steel slag as supplementary cementitious material. *Construction and building materials*, 449, 138566. <https://doi.org/10.1016/j.conbuildmat.2024.138566>

- [30] Krishnan, S., Kanaujia, S. K., Mithia, S., & Bishnoi, S. (2018). Hydration kinetics and mechanisms of carbonates from stone wastes in ternary blends with calcined clay. *Construction and building materials*, 164, 265–274. <https://doi.org/10.1016/j.conbuildmat.2017.12.240>
- [31] Wang, L., Ren, Z., Wang, H., Liang, X., Liu, S., Ren, J., ... & Zhang, M. (2022). Microstructure-property relationships in cement mortar with surface treatment of microbial induced carbonate precipitation. *Composites part b: Engineering*, 239, 109986. <https://doi.org/10.1016/j.compositesb.2022.109986>
- [32] Li, J., Mao, J., & Zhang, G. (2011, July). Multi-performance optimization of cement blending process. *Proceedings of the 30th chinese control conference* (pp. 1877-1881). IEEE. <https://ieeexplore.ieee.org/abstract/document/6000603>
- [33] Collivignarelli, M. C., Cillari, G., Ricciardi, P., Miino, M. C., Torretta, V., Rada, E. C., & Abbà, A. (2020). The production of sustainable concrete with the use of alternative aggregates: A review. *Sustainability*, 12(19), 7903. <https://doi.org/10.3390/su12197903>
- [34] Lothenbach, B., Scrivener, K., & Hooton, R. D. (2011). Supplementary cementitious materials. *Cement and concrete research*, 41(12), 1244-1256. <https://doi.org/10.1016/j.cemconres.2010.12.001>
- [35] Marvila, M T., Azevedo, ARG., & Vieira, CMF. (2021). Reaction mechanisms of alkali-activated materials. *Revista ibracon de estruturas e materiais*, 14(3), e14309. <https://doi.org/10.1590/S1983-41952021000300009>
- [36] Gunzel, F. S. (2021). *3D printing of rapid setting ordinary concrete mixtures* [Thesis]. <https://scholar.sun.ac.za/items/05000803-e186-49c8-b16b-48554c885870>
- [37] Fode, T A., Jande, YAC., & Kivevele, T. (2023). Effects of different supplementary cementitious materials on durability and mechanical properties of cement composite—Comprehensive review. *Heliyon*, 9(7), e17924. <https://doi.org/10.1016/j.heliyon.2023.e17924>
- [38] Heikal, M., Nassar, M. Y., El-Sayed, G., & Ibrahim, S. M. (2014). Physico-chemical, mechanical, microstructure and durability characteristics of alkali activated Egyptian slag. *Construction and building materials*, 69, 60–72. <https://doi.org/10.1016/j.conbuildmat.2014.07.026>
- [39] Negrin, I., Kripka, M., & Yepes, V. (2023). Multi-criteria optimization for sustainability-based design of reinforced concrete frame buildings. *Journal of cleaner production*, 425, 139115. <https://doi.org/10.1016/j.jclepro.2023.139115>
- [40] Yurt, Ü. (2020). High performance cementless composites from alkali activated GGBFS. *Construction and building materials*, 264, 120222. <https://doi.org/10.1016/j.conbuildmat.2020.120222>
- [41] Li, Z., Gao, X., Lu, D., & Dong, J. (2022). Early hydration properties and reaction kinetics of multi-composite cement pastes with supplementary cementitious materials (SCMs). *Thermochimica acta*, 709, 179157. <https://doi.org/10.1016/j.tca.2022.179157>
- [42] Golubchikov, O., & Badyina, A. (2012). *Sustainable housing for sustainable cities: a policy framework for developing countries*. <https://api.semanticscholar.org/CorpusID:16860664>
- [43] Wang, J., Huang, T., Han, L., Xie, F., Liu, Z., & Wang, D. (2021). Optimization of alkali-activated concrete based on the characteristics of binder systems. *Construction and building materials*, 300, 123952. <https://doi.org/10.1016/j.conbuildmat.2021.123952>
- [44] Arbi, K., Nedeljkovic, M., Zuo, Y., & Ye, G. (2016). A review on the durability of alkali-activated fly ash/slag systems: Advances, issues, and perspectives. *Industrial & engineering chemistry research*, 55(19), 5439–5453.
- [45] Ma, G., Zhang, J., Wang, L., Li, Z., & Sun, J. (2018). Mechanical characterization of 3D printed anisotropic cementitious material by the electromechanical transducer. *Smart materials and structures*, 27(7), 75036. <https://doi.org/10.1088/1361-665X/aac789>
- [46] Ahmed, Z. Y., Bos, F. P., Wolfs, R. J., & Salet, T. A. (2016). Design considerations due to scale effects in 3D concrete printing. *8th international conference of the arab society for computer aided architectural design* (pp. 115-124). [https://papers.cumincad.org/data/works/att/ascaad2016\\_001.pdf#page=126](https://papers.cumincad.org/data/works/att/ascaad2016_001.pdf#page=126)
- [47] Olafusi, O. S., Sadiku, E. R., Snyman, J., Ndambuki, J. M., & Kupolati, W. K. (2019). Application of nanotechnology in concrete and supplementary cementitious materials: A review for sustainable construction. *SN applied sciences*, 1(6), 580. <https://doi.org/10.1007/s42452-019-0600-7>
- [48] Sutter, L. L., & Hooton, R. D. (2023). Progress towards sustainability through performance-based standards and specifications. *Cement and concrete research*, 174, 107303.
- [49] Joensuu, T., Edelman, H., & Saari, A. (2020). Circular economy practices in the built environment. *Journal of cleaner production*, 276, 124215. <https://doi.org/10.1016/j.jclepro.2020.124215>